PB88-201199

Kinetics and Selectivity of Deep Catalytic Oxidation of n-Hexane and Benzene

(U.S.) Environmental Protection Agency
Research Triangle Park, NC

1988

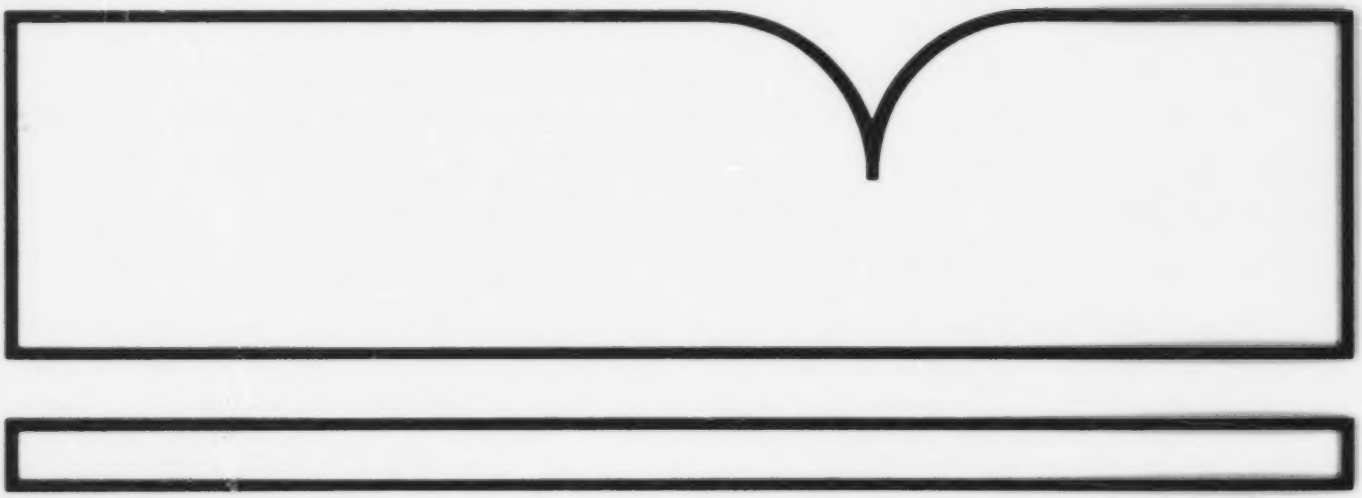

U.S. Department of Commerce
National Technical Information Service
NTIS

EPA/600/J-88/008
JOURNAL ARTICLE

Applied Catalysis, 36 (1988) 231-247
Elsevier Science Publishers B.V., Amsterdam — Printed in The Netherlands

Kinetics and Selectivity of Deep Catalytic Oxidation of n-Hexane and Benzene

S.K. GANGWAL*, M.E. MULLINS, J.J. SPIVEY and P.R. CAFFREY

Research Triangle Institute, P.O. Box 12194, Research Triangle Park, NC 27709 (U.S.A.)

and

B.A. TICHENOR

U.S. Environmental Protection Agency, Air and Energy Engineering Research Laboratory, Research Triangle Park, NC 27711 (U.S.A.)

(Received 12 February 1987, accepted 24 August 1987)

ABSTRACT

Deep (complete) catalytic combustion (oxidation) of volatile organic compounds (VOCs) is emerging as an important emission control technique. A fundamental study was carried out for low-temperature deep oxidation of n-hexane and benzene over a 0.1% Pt, 3% Ni/γ-Al_2O_3 catalyst. These VOCs were subjected to oxidation as single components and as a binary mixture at temperatures ranging from 160 to 360°C. n-Hexane oxidation was significantly inhibited in the mixtures. An approach based on the Mars-Van Krevelen rate model was used to explain the results. Kinetic parameters were developed for the individual VOCs based on single component differential reactor data. These kinetic parameters were then incorporated into a proposed multicomponent Mars-Van Krevelen rate model to predict the experimental conversions in the binary mixture. The model was found to be reasonably successful in predicting the conversion of benzene and n-hexane in their binary mixture.

INTRODUCTION

The subject of heterogeneous catalytic oxidation of organic compounds in the vapor phase has been reviewed by various authors (Prasad et al. [1], Golodets [2], Butt [3], Margolis [4], Germain [5], Cullis [6], Dixon and Longfield [7]). From an industrial perspective, two different types of heterogeneous catalytic oxidation processes may be recognized: (i) partial oxidation for manufacturing of commercially significant products (e.g., ethylene to ethylene oxide, benzene to maleic anhydride, and naphthalene to phthalic anhydride) and (ii) deep (or complete) oxidation of trace (low-concentration) organic contaminants in air (e.g., for air purification, industrial emission control, and automotive exhaust catalysis). The low-temperature, deep oxidation of trace

0166-9834/88/$03.50 © 1988 Elsevier Science Publishers B.V.

NTIS is authorized to reproduce and sell this report. Permission for further reproduction must be obtained from the copyright owner.

organic contaminants, referred to as volatile organic compounds (VOCs) herein, is the subject of this paper. Deep oxidation is carried out using highly active, non-selective catalysts containing either noble metals (Pt, Pd, Rh), oxides of base metals (Co, Ni, Mn), or various combinations of these materials. The temperature range of primary interest to this study is 140–360°C.

Reported applications for deep catalytic oxidation include odor removal from sewage pumping off-gases (Bonnaci and Heck [8]), polymer-processing vapor control (Budd [9]), odor control from coffee-roasting gases (Balough et al. [10]), and solvent emission abatement in automotive spray painting (Roberts and Roberts [11]). Commercial systems are usually designed to accomplish complete oxidation of the compound in the stream that is most difficult to oxidize or that is of most environmental concern. Because the compositions of the gas streams containing the oxidizable compounds are very complex, the overall performance of these field systems is reported in terms of gross parameters, such as "odor reduction" or "percent carbon removal", and do not allow evaluation of the effect of the presence of any one compound in the oxidizable mixture on the oxidation of other compounds. On the other hand, reported fundamental research studies are generally for single compounds only (Golodets [2]).

Thus, there is a dearth of fundamental work in the reported literature focusing on deep catalytic oxidation of a mixture of VOCs. In general, catalyst selection for purification of air containing a mixture of VOCs is based on determination of catalyst activity for single compounds in the input air (Christian and Johnson [12], Johns [13], Miller and Piatt [14], Rousseau [15]). However, as pointed out by Musick et al. [16], such determinations cannot be expected to show the possible effects of the simultaneous presence of a multitude of compounds. The fundamental investigation of these "mixture effects" is of primary interest in this paper.

In recent years, research to investigate the effectiveness of deep catalytic oxidation over a range of operating conditions and emission-stream characteristics (Martin [17], Jennings [18]) has emphasized the catalytic oxidation of total VOCs, rather than individual VOCs, in the mixtures. In more recent studies (Palazzolo et al. [19], Tichenor and Palazzolo [20]), the emphasis has been on oxidation of the individual VOCs in the mixtures being oxidized. In both of these studies, a pilot-scale catalytic incinerator (platinum–palladium catalyst on a ceramic honeycomb substrate) was operated at temperatures ranging from 260 to 425°C and space velocities ranging from 15 000 to 80 000 h^{-1}. Eight multi-component VOC mixtures with 2–7 VOCs in each mixture were tested. In addition, 16 of the VOCs were tested singly. These tests showed that a compound may behave quite differently when oxidized in a mixture versus when oxidized as a single compound. For example, n-hexane oxidation was inhibited in mixtures, whereas ethyl acetate oxidation was enhanced in mixtures.

Other past studies of the oxidation of a compound by itself and in a mixture

generally show that mixtures inhibit the oxidation of the compound of interest, with few exceptions. Yao and Kummer [21] studied the oxidation of ethene, propene, ethane, propane and carbon monoxide over nickel oxide crystals. The olefins were retarded much less than the alkanes. The authors have attempted to explain their results by competition among the hydrocarbons for adsorbed oxygen or for undefined adsorption sites. Cullis et al. [22] studied the oxidation of methane over a Pd/Al_2O_3 catalyst in the presence of propane, methanol, formaldehyde, and dichloromethane. All these compounds retarded methane oxidation. Propane was oxidized very little compared to formaldehyde and methanol. Dichloromethane inhibited deep oxidation but enhanced partial oxidation of methane to formaldehyde. Musick et al. [16] carried out oxidation experiments involving carbon monoxide, hydrogen, methane, propane, benzene, thiophene, and monochlorodifluoromethane over a copper–manganese oxide catalyst (hopcalite), a supported hopcalite containing 0.02% palladium, and a supported platinum catalyst (0.5% platinum on alumina) in the presence of humidified air at 315 °C and 21 000 h^{-1} space velocity. This study evaluated either carbon monoxide by itself or carbon monoxide mixed with one or more of the other compounds. Benzene inhibited carbon monoxide oxidation, whereas thiophene partially poisoned the catalysts in addition to inhibiting carbon monoxide oxidation. The poisoning of the catalyst and inhibition of carbon monoxide oxidation due to thiophene appeared to proceed as independent phenomena, as evidenced by the partial recovery of catalyst activity when thiophene was taken off stream. The catalytic activity for carbon monoxide oxidation was inhibited by all compounds except methane on the hopcalite catalyst and was uninhibited by all compounds except hydrogen on the platinum catalyst. Interestingly, methane slightly enhanced carbon monoxide oxidation on the hopcalite catalyst.

In addition to purely kinetic effects at low to moderate temperatures, the interpretation of data on mixture effects may be further complicated by mass transfer effects at higher temperatures. The long-term objective of this study is to gain a fundamental understanding of mixture effects in deep catalytic oxidation of VOC mixtures containing organic compounds of different classes. This paper presents initial results of this ongoing study of oxidation of mixtures containing n-hexane and benzene over a commercial 0.1% Pt, 3% Ni/γ-Al_2O_3 catalyst.

EXPERIMENTAL

Chemicals and catalyst

Benzene and n-hexane premixed with hydrocarbon free, dry air in gas cylinders at concentrations ranging from 10 to 600 ppmv hydrocarbon were obtained from Scott Specialty Gases, Plumsteadville, PA, U.S.A. A number of

TABLE 1

Test gas mixtures

	Concentration in air (ppmv)
Single hydrocarbon	
Benzene	9, 69, 163, 375, 525
n-Hexane	201, 410, 566
Binary mixture	
Benzene + n-Hexane	189 + 190

gases containing single components and a binary benzene-n-hexane mixture were obtained, as shown in Table 1.The gases were used one at a time in the deep-oxidation experiments.

The catalyst was obtained from United Catalyst, Louisville, KY, U.S.A. as 1/4-in. (6.35-mm) cylinders. The commercial designation of the catalyst was G-43, and its nominal composition as supplied by the vendor was 0.1% Pt, 3% Ni/γ-Al_2O_3. The catalyst was crushed and screened to two different particle sizes (120×170 and 60×80 mesh) prior to use in the oxidation experiments.

Apparatus

A laboratory-scale microreactor system, shown in Fig. 1, was used for all the experiments. The premixed gas was delivered using a two-stage pressure regulator with the gas-flow split into two equal flows using two differential flow controllers as shown. One flow stream was passed through the microreactor, whereas the other was passed through a bypass line. The reactor consisted of a 60-cm-long Pyrex™ tube (6 mm O.D., 4 mm I.D. for the 60×80 mesh catalyst; 3 mm O.D., 1.5 mm I.D., for the 120×170 mesh catalyst), and the catalyst was positioned at the center of the tube using fine Pyrex wool plugs. The tube was surrounded by a three-zone 45-cm-long split tube furnace. The end zones were each 7.5 cm long, and the central zone was 30 cm long. The temperature of each heating zone was controlled separately using proportional temperature controllers. Four 0.5 mm O.D. measurement thermocouples (type K) were mounted, equally spaced, along the small catalyst bed to ensure temperature uniformity. The temperature control was better than ± 0.5°C in each zone. After the two split gas streams flowed through the reactor and the bypass line, they entered a thermostated Valco ten-port gas sampling valve maintained at 100°C for sequential sampling of the reactor outlet stream and the bypass stream (i.e., representative of the reactor inlet stream) using two identical 0.25-cm^3 sample loops.

The samples were injected automatically, using a Carle Valve Minder consisting of a valve actuator and a valve timer, into a Varian 3700 gas chroma-

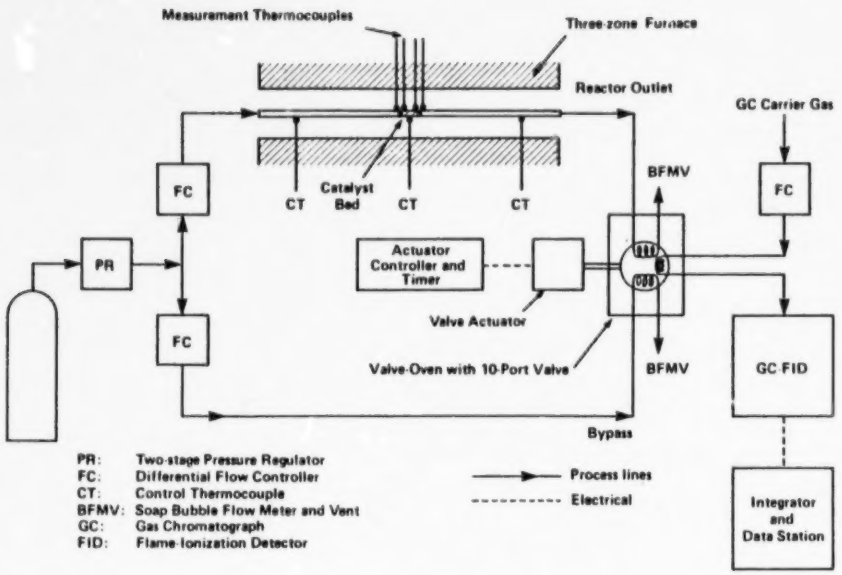

Fig. 1. Microreactor system.

tograph equipped with a flame ionization detector. A 5 ft. (1.5 m) × 1/8 in. (3 mm) stainless-steel column consisting of 3% SP 1500 on 18–120 mesh Carbopack B was used for the separation and analysis of the hydrocarbons isothermally at 140 °C. A complete analysis of the three hydrocarbons of interest could be performed in 4.5 min. The valve timer was placed on a 9-min cycle to allow the measurement of the hydrocarbons in the reactor inlet and in the reactor outlet streams sequentially. Because the inlet concentration of the gas stream was a known constant, the outlet concentration was obtained assuming a linear response of the flame ionization detector with respect to the inlet concentration for the hydrocarbons of interest. The analysis of the inlet during every cycle was extremely important because of variation of the detector response during the course of a typical day of the experiment. Even though the detector response may have drifted or cycled during the day, it would affect the outlet and the inlet stream concentrations in a fixed ratio. Thus, the sampling procedure allowed accurate measurement of the reactor outlet concentrations, irrespective of the drift in the detector response. The peak areas were measured electronically using a Perkin-Elmer Sigma 10B data station. The bypass and reactor outlet gas flows were measured using a soap bubble flow meter to ensure that they were equal. This equality of flow was necessary for accurate determination of the reactor outlet concentration.

Procedure

All experiments were carried out at temperatures ranging from 140 to 360°C and a weight hourly space velocity (WHSV) ranging from 50 to 1000. A 17-mg catalyst bed was used for the 120×170 mesh particles, and a 20-mg catalyst bed was used for the 60×80 mesh particles. The experimental procedure consisted of measuring the reactor inlet and outlet concentrations at a series of constant temperatures and gas-flow rates for each gas. Extensive preliminary experiments were initially carried out at a range of space velocities for the two catalyst particle sizes. These experiments firmly established the absence of mass transfer effects above a WHSV of 200 at temperatures below 200°C for the 120×170 mesh particles. Integral reactor high-conversion experiments were then carried out at a WHSV of 209 for the entire temperature range of interest using the120×170 mesh catalyst. Single-component gases were run first followed by the binary mixture. These experiments allowed us to establish whether mixture effects were present to a significant degree. More fundamental differential reactor experiments (less than 10 percent conversion) were then carried out for each pure component in the surface reaction controlled region (<220°C) to evaluate its rate expression. These rate expressions are used to explain the results of the integral reactor experiments and to evaluate mixture effects.

RESULTS

During initial exposure of the 0.1% Pt, 3% Ni/γ-Al_2O_3 catalyst to a hydrocarbon (VOC) containing air stream at approximately 315°C, the catalyst exhibited a prolonged induction period (up to 72 h), during which catalyst activity increased by nearly two orders of magnitude. The catalyst activity increased further at a higher operating temperature (365°C) until a very stable activity level was reached. All results presented are for a catalyst at this steady-state activity, which remained constant throughout the duration of the reported experiments (approximately 3 months). The induction period experiments and results will be discussed in a later paper.

Figs. 2 and 3 show the conversion data for n-hexane and benzene as a function of temperature. All these results were obtained at an identical WHSV of 209. As shown in Fig. 2, the conversion of n-hexane is significantly inhibited in the binary mixture versus as a single component. From Fig. 3, the conversion of benzene appears to be nearly unaffected in the binary mixture; however, its rate is inhibited as discussed in the next paragraph. In order to explain the results in Figs. 2 and 3, it was deemed necessary to obtain intrinsic kinetic rates for the two components individually. This was done by operating the reactor as a differential reactor for the two components individually at a series of concentrations and temperatures. The conversions were maintained be-

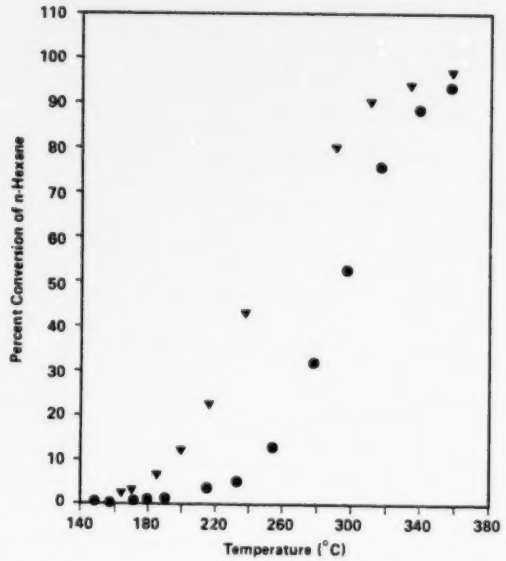

Fig. 2. Effect of n-hexane–benzene mixture on n-hexane conversion. Catalyst: 17 mg, 120×170 mesh. WHSV = 209. Key: (▼) 410 ppm n-hexane in air; (●) 190 ppm n-hexane with 189 ppm benzene in air.

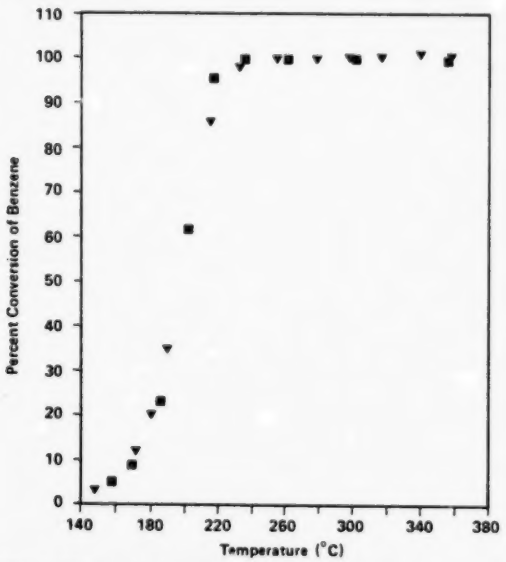

Fig. 3. Effect of n-hexane–benzene mixture on benzene conversion. Catalyst and WHSV as in Fig. 2. Key: (■) 375 ppm benzene in air; (▼) 189 ppm benzene with 190 ppm n-hexane in air.

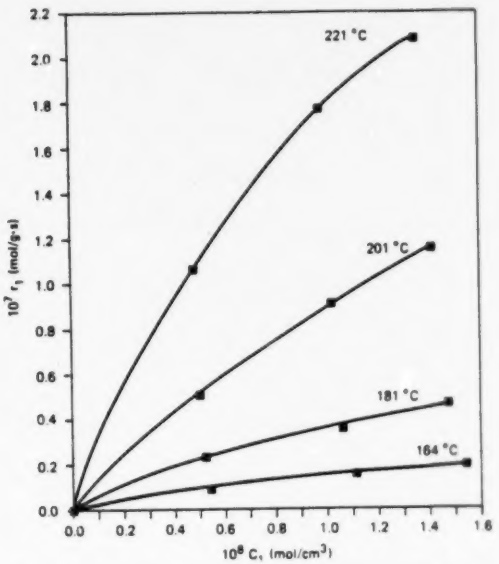

Fig. 4. Differential reaction rate for n-hexane oxidation.

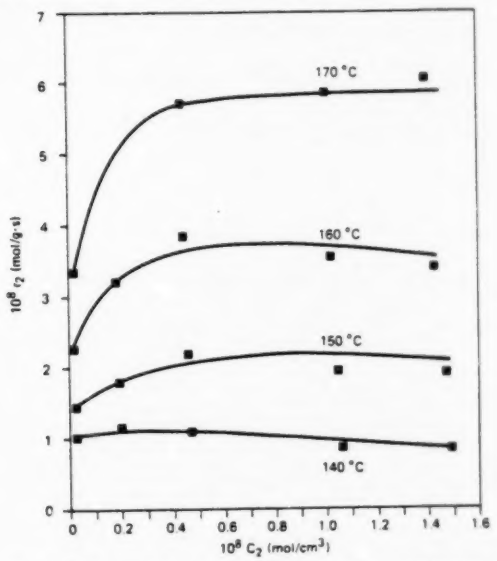

Fig. 5. Differential reaction rate for benzene oxidation.

tween 5 and 8% by adjusting WHSV. The temperatures chosen were generally below 220°C to ensure that data were obtained in the surface kinetic region.

The rate data as a function of temperature and concentration are shown in Fig. 4 and 5 for n-hexane and benzene, respectively. n-Hexane exhibits close to first-order behavior at temperatures up to 201°C (Fig. 4). On the other hand, benzene exhibits close to zero-order behavior at all temperatures tested, at concentrations above about $4 \cdot 10^{-9}$ mol/cm^3. The zero-order behavior of benzene clearly demonstrates rate inhibition in the mixture for benzene (Fig. 3) even though the conversion appears unaffected. If there were no inhibitions, the conversion of benzene in the mixture should have been higher than those measured since the inlet concentration of benzene is lower in the mixture than as a single component. We may fit an empirical power law kinetic expression to the differential data for n-hexane and assume a zero-order behavior for benzene. Although these kinetic expressions would represent single-component behavior accurately in the intrinsic kinetic region, they would not be useful for explaining the complex interactions observed in the catalytic oxidation of mixtures. A more rigorous approach is to develop kinetic expressions involving surface interactions (e.g., Langmuir–Hinshelwood, Eley–Rideal, or Mars–Van Krevelen) because they may allow explanation of the complex interactions, e.g., via competitive adsorption. This approach has been adopted and is detailed in the next section of this paper.

DISCUSSION

Mechanistic kinetic expressions are needed to represent the rate data obtained in Figs. 4 and 5 and to explain quantitatively the effects observed in Figs. 2 and 3. The mechanistic kinetic model that has received the widest support (Balasubramanian and Viswanath [23], Golodets [2], Jaswal et al. [24]) for the oxidation of organic compounds is due to Mars and Van Krevelen [25] and is:

$$R_i + \text{oxidized catalyst} \xrightarrow{k_i} \text{reduced catalyst} + \text{products}$$

$$O_2 + \text{reduced catalyst} \xrightarrow{k_{O_i}} \text{oxidized catalyst}$$

In this mechanism, the above steps are assumed to be first-order in the respective gaseous species. Thus, if θ is the fraction of oxidized catalyst at any time, then:

$$r_i = k_i \, C_i \, \theta \tag{1}$$

and

$$r_{o_2} = k_{o_i} \, C_o (1 - \theta) \tag{2}$$

If stoichiometry for oxidation requires γ_i moles of oxygen per mole of carbon, then:

$$r_{o2} = \gamma_i \, r_i \tag{3}$$

from eqns. 1, 2, and 3, eliminating θ,

$$r_i = \frac{k_{o_i} \, k_i \, C_o \, C_i}{k_{o_i} \, C_o + \gamma_i k_i C_i} \tag{4}$$

which is the Mars and Van Krevelen [25] rate expression for oxidation of hydrocarbon species i. Note that the apparent experimentally observed order of the hydrocarbon oxidation rate with respect to the hydrocarbon species varies between the extremes of 0 and 1. When

$$k_{o_i} \, C_o \gg \gamma_i \, k_i \, C_i$$

then

$$r_i \approx k_i \, C_i \text{ (first-order with respect to hydrocarbon)}, \tag{5}$$

and when

$$k_{o_i} \, C_o \ll \gamma_i \, k_i \, C_i$$

then

$$r_i \approx \frac{k_{o_i} \, C_o}{\gamma_i} \text{ (zero-order with respect to hydrocarbon)}. \tag{6}$$

The next step is to evaluate the respective k values for the components of interest, i.e., n-hexane and benzene. This may be facilitated by inverting eqn. 4:

$$\frac{1}{r_i} = \frac{1}{k_i} \frac{1}{C_i} + \frac{\gamma_i}{k_{o_i} \, C_o} \tag{7}$$

Because in our experiments C_o is nearly a constant due to the large excess of oxygen, eqn. 7 should be a nearly linear relationship between inverse reaction rate and inverse concentration if eqn. 4 adequately represents the oxidation rate data. Plots for $1/r_i$ versus $1/C_i$ for n-hexane are shown in Fig. 6 at several temperatures. The linearity of these plots lends credence to the Mars–Van Krevelen mechanism for n-hexane. Arrhenius relationships and plots for the corresponding k values are shown in Fig. 7.

A problem is encountered if a similar approach is attempted for benzene because benzene exhibits nearly a zero-order behavior at concentrations greater than $4 \cdot 10^{-9}$ mol/cm^3 (Fig. 5). The limiting zero-order relationship is given by eqn. 6, which may be used to evaluate k_{o_i} for benzene as a function of temperature from rate data in the nearly horizontal portions of the plots in Fig. 6.

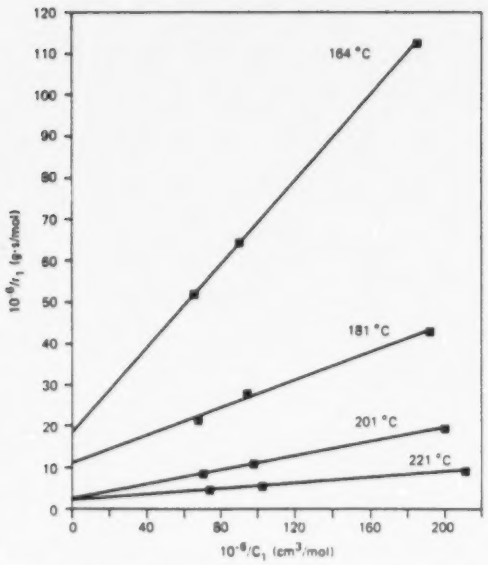

Fig. 6. Inverse reaction rate versus inverse concentration for n-hexane oxidation.

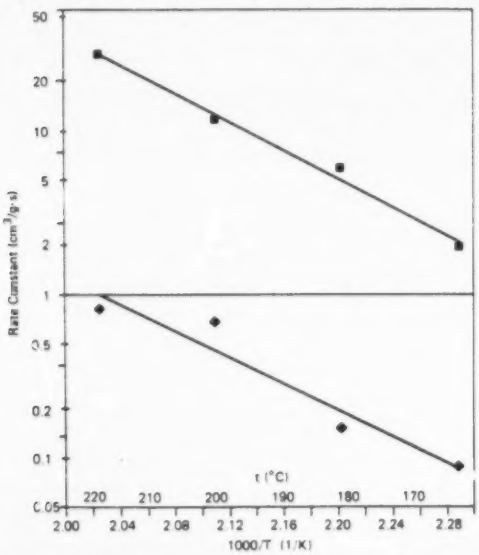

Fig. 7. Mars-Van Krevelen [25] rate constants for n-hexane oxidation. $k_1 = 1.66 \cdot 10^{10}$ exp $(-82\,763/RT)$, correlation coefficient = 0.995. $k_0 = 1.75 \cdot 10^{8}$ exp $(-77\,905/RT)$, correlation coefficient = 0.964.

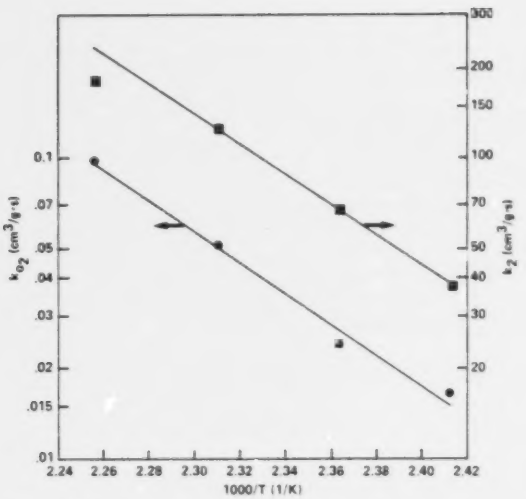

Fig. 8. Mars-Van Krevelen [25] rate constants for benzene oxidation. $k_2 = 5.347 \cdot 10^{13}$ exp $(-96\,351/RT)$ correlation coefficient = 0.998 (three lower phases). $k_{o_2} = 3.41 \cdot 10^{10}$ exp $(-97\,939/RT)$, correlation coefficient = 0.995.

k_i for benzene may be evaluated using the data at the lowest concentration from the limiting first-order eqn. 5. Arrhenius plots for k_i and k_{o_i} evaluated in this manner are shown in Fig. 8. Only the three lowest temperatures have been used to evaluate k_i because it was not possible, because of experimental limitations, to obtain the data at the highest temperature under true differential reactor conditions.

The complete Mars–Van Krevelen [25] formulations for the components for oxidation as single components are summarized in Table 2. To apply these relationships to the mixture effects shown in Figs. 2 and 3, a multicomponent

TABLE 2

Mars-Van Krevelen [25] rate equation parameters

$$r_i = \frac{k_{o_i}\, k_i\, C_o\, C_i}{k_{o_i}\, C_o + \gamma_i\, k_i\, C_i}$$

	$k_{o_i}, \left(\frac{\text{cm}^3}{\text{g}\cdot\text{s}}\right)$	$k_i, \left(\frac{\text{cm}^3}{\text{g}\cdot\text{s}}\right)$	γ_i (—)
n-Hexane	$1.75 \cdot 10^8 \exp\,[-77\,905/RT]$	$1.66 \cdot 10^{10} \exp\,[-82\,763/RT]$	9.5
Benzene	$3.41 \cdot 10^{10} \exp\,[-97\,939/RT]$	$5.347 \cdot 10^{13} \exp\,[-96\,351/RT]$	7.5

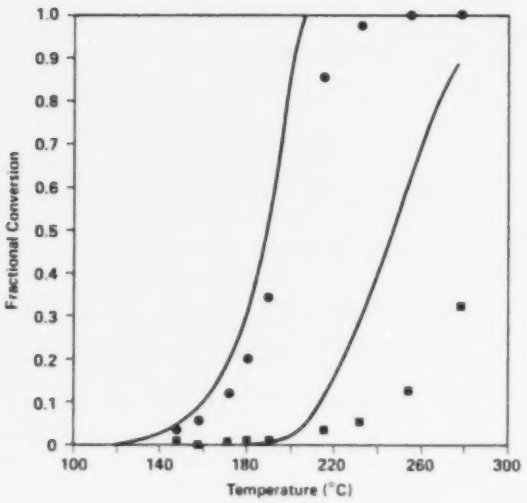

Fig. 9. Comparison of predicted (—) and actual conversions for benzene and n-hexane in a binary mixture. Inlet composition: 189 ppm benzene (●) and 190 ppm n-hexane (■). WHSV = 209.

model needs to be postulated based on the Mars–Van Krevelen mechanism. Because the reoxidation rate constants (k_{o_i} values) for benzene and n-hexane are different, it is reasonable to assume that the catalytic species is reduced to different oxidation states. n-Hexane and benzene as R_1 and R_2, respectively, are designated. Then, for oxidation of a mixture of these hydrocarbons, the following may be postulated:

$$R_1 + \text{oxidized catalyst} \xrightarrow{k_1} [\text{reduced catalyst}]_1 + \text{products} \tag{8}$$

$$O_2 + [\text{reduced catalyst}]_1 \xrightarrow{k_{o_1}} \text{oxidized catalyst} \tag{9}$$

$$R_2 + \text{oxidized catalyst} \xrightarrow{k_2} [\text{reduced catalyst}]_2 + \text{products} \tag{10}$$

$$O_2 + [\text{reduced catalyst}]_2 \xrightarrow{k_{o_2}} \text{oxidized catalyst} \tag{11}$$

If at any instant θ_1 and θ_2 are the fractions of the catalyst surface occupied by $[\text{reduced catalyst}]_1$ and $[\text{reduced catalyst}]_2$, respectively, then the following balances may be written:

$$r_1 = k_i C_i (1-\theta_1 - \theta_2) = \gamma_1 k_{o_1} C_o \theta_1 \tag{12}$$

$$r_2 = k_2 C_2 (1-\theta_1 - \theta_2) = \gamma_2 k_{o_2} C_o \theta_2 \tag{13}$$

θ_1 and θ_2 may be evaluated from eqns. 12 and 13 and substituted in the right-hand sides of these equations to yield the respective rate equations for oxidation in a binary mixture:

$$r_1 = \frac{k_{o_1} k_1 C_o C_1}{k_{o_1} C_o + \gamma_1 k_1 C_1 + \gamma_2 \left(\frac{k_{o_1}}{k_{o_2}}\right) k_2 C_2} \tag{14}$$

$$r_2 = \frac{k_{o_2} k_2 C_o C_2}{k_{o_2} C_o + \gamma_2 k_2 C_2 + \gamma_1 \left(\frac{k_{o_2}}{k_{o_1}}\right) k_1 C_1} \tag{15}$$

A general rate form for deep oxidation of the ith component in an n-component mixture may be easily inferred from eqns. 14 to 15:

$$r_i = \frac{k_{o_i} k_i C_o C_i}{k_{o_i} C_o + \sum_{j=1}^{n} \frac{k_{o_i}}{k_{o_j}} \gamma_j k_j C_j}, \; i = 1,2....n \tag{16}$$

Using single-component rate data (Table 2), eqn. 16 may be used to predict the conversion of each hydrocarbon component in a mixture in the intrinsic kinetic region. If such a multicomponent model is credible, then the predicted conversions would require setting up component balances for each species. Because a tubular reactor has been used in our experiments, the rate of reaction changes along the bed since the concentrations change along the bed. Thus, differential component balances (assuming plug flow) have been set up as follows for an n-component mixture:

$$\frac{d f_i}{dw} = \frac{r_i}{v_o C_{io}}, \; i = 1,2,....n \tag{17}$$

with inlet boundary condition, $f_i(0) = 0, \; i = 1,2,...n$ (18)

where f_i is the fractional conversion of species i and w is the catalyst weight.

The n-coupled ordinary nonlinear first-order differential equations for an n-component mixture must be solved simultaneously using a suitable numerical technique. A fourth-order Runge–Kutta method has been used to solve these equations and to evaluate conversions of benzene and n-hexane in their binary mixture. The model evaluations for the binary mixture are compared to the actual experimental results (from Figs. 2 and 3) in Fig. 9.

From Fig. 9, the model makes reasonable predictions of n-hexane conversion up to about 200 °C, beyond which it begins to overpredict. The degree of overprediction increases with increase in temperature. The model somewhat overpredicts benzene conversion throughout the temperature range. The overprediction of n-hexane begins to rapidly increase at the point where ben-

zene is nearly completely consumed as predicted by the model. The reason for this is that the magnitude of the denominator (adsorption term) of eqn. 16 strongly affects the rate of either component and is a function not only of the rate constants but also of the concentrations. Since benzene is overpredicted in the kinetic region, the magnitude of the adsorption term for benzene must be actually somewhat greater than that given by the proposed multicomponent Mars–Van Krevelen model. A more rigorous model is thus needed which results in a larger adsorption term for benzene. This might be accounted for by including an adsorption term for water. This will reduce benzene conversion and thereby more correctly predict n-hexane conversion as well at the higher temperatures. At the higher temperatures, the increase in overprediction may also be caused by pore diffusion or external diffusion effects. We are currently attempting to refine the reactor model to include these mass-transfer effects. This would require formulation and simultaneous numerical solution of particle differential equations along with the gas phase equations.

CONCLUSIONS

Based on the work to date, we may draw the following conclusions:

(1) Deep catalytic oxidation rates of benzene and n-hexane in their binary mixture are lower than when the hydrocarbons are present by themselves.

(2) The Mars–Van Krevelen mechanism appears to be an adequate representation for deep catalytic oxidation of benzene and n-hexane when present by themselves.

(3) A simple multicomponent kinetic model (eqns. 8–11) based on the Mars–Van Krevelen mechanism made reasonable predictions of experimental data for binary n-hexane/benzene mixture, but needs to be refined further.

(4) Refinement of the kinetic model should involve development of a model which gives a bigger adsorption term for benzene in the mixture and incorporates diffusional effects.

NOMENCLATURE

			Units
C_i	=	hydrocarbon (VOC) concentration	mol/cm^3
C_{io}	=	inlet hydrocarbon (VOC) concentration	mol/cm^3
C_o	=	oxygen concentration	mol/cm^3
f_i	=	fractional conversion of species i	– –
k_i	=	surface reduction rate constant for species i	$cm^3/(g \cdot s)$
k_{o_i}	=	surface reoxidation rate constant for species i	$cm^3/(g \cdot s)$
R	=	gas constant, 8.314	$J/(mol \cdot K)$
R_i	=	hydrocarbon species, i	– –
r_i	=	rate of oxidation of species i	$mol/(g \cdot s)$
r_{o_2}	=	rate of oxygen consumption	$mol/(g \cdot s)$

T	=	absolute temperature	K
t	=	temperature	°C
v_o	=	volumetric flow-rate at reaction temperature	cm^3/s
w	=	catalyst weight	g
WHSV	=	weight hourly space velocity	g gas/(g catalyst·h)

Greek symbols

γ_i	=	stoichiometric coefficient for deep oxidation of species i	--
θ	=	fraction of oxidized catalyst	--
θ_1,θ_2	=	fraction of reduced catalyst corresponding to n-hexane and benzene, respectively	--

ACKNOWLEDGEMENTS

Financial support for this work was provided by the U.S. Environmental Protection Agency and the U.S. Air Force under EPA Cooperative Agreement No. CR812522-01-0 and U.S. Air Force Interagency Agreement No. RW57931254.

REFERENCES

1 R. Prasad, L.A. Kennedy and E. Ruckenstein, Catal. Rev. Sci. Eng., 26 (1984) 1.
2 G.I. Golodets, Heterogeneous Catalyst Reactions Involving Molecular Oxygen, Elsevier, New York, Part III, 1983, p. 396.
3 J.B. Butt, AIChE J., 22 (1976) 1.
4 L.Ya. Margolis, Catal. Rev., 8 (1973) 241.
5 J.E. Germain, Catalytic Conversion of Hydrocarbons, Academic Press, London, 1969, Ch. 5, p. 231.
6 C.F. Cullis, Ind. Eng. Chem., 59:12 (1967) 18.
7 J.K. Dixon and O.E. Longfield, in P.H. Emmett (Editor), Catalysis, Vol. 7, Reinhold, New York, 1960, Ch. 3, p. 183.
8 J.C. Bonnaci and R.M. Heck, Pollution Control Catalytic Equipment, paper presented at the International Precious Metals Institute Seminar, The Platinum Group Metals — an In-Depth View of the Industry, Williamsburg, VA, April 10–13, 1983.
9 A.E.R. Budd, Environ. Pollut. Manage., Jan./Feb. (1978) 13.
10 A. Balough, J. Herendi and J. Bathory, Catalytic Purification of Gaseous Factory Effluents to Protect the Environment, National Technical Information Service, Springfield, VA Report No. AD-A017 807, 1975.
11 R.E. Roberts and J.B. Roberts, J. Air Pollut. Contr. Assoc., 26 (1976) 353.
12 J.G. Christian and J.E. Johnson, Int. J. Air Water Pollut., 9 (1965) 1.
13 R. Johns, Chem. Eng. Progr. Symp. Ser., 62:63 (1966) 81.
14 R.R. Miller and V.R. Piatt (Editors), The Present Status of Chemical Research in Atmosphere Purification and Control, Naval Research Laboratory Report 5465, April 21, 1960, Washington, DC, Chs. 7 and 8, p. 67. April 21, 1960.
15 J. Rousseau, Atmospheric Control Systems for Space Vehicles, U.S. Air Force Report ASD-TDR-62-527, Part II, AiResearch Mfg. Co., February 1964, p. 93.

16 J.K. Musick, F.S. Thomas and J.E. Johnson, Ind. Eng. Chem. Proc. Des. Develop., 1 (1972) 350.
17 N.A. Martin, Catalytic Incineration of Low Concentration Organic Vapors, Report No. EPA-600/2-81-017 (NTIS No. PB81-158446), U.S. Environmental Protection Agency, Research Triangle Park, NC, February 1981.
18 M.S. Jennings, Control of Industrial VOC Emissions by Catalytic Incineration, Vols. 1-9, Report Nos. EPA-600/2-84-118a-i (NTIS Nos. PB84-225762, -225770, -225788, -225796, -103199, -225812, -103173, -103181, and -225846), U.S. Environmental Protection Agency, Research Triangle Park, NC, July 1984.
19 M.A. Palazzolo, J.I. Steinmetz, D.L. Lewis and J.F. Beltz, Parametric Evaluation of VOC/HAP Destruction Via Catalytic Incineration, Report No. EPA-600/2-85-041 (NTIS No. PB85-191187/A7), U.S. Environmental Protection Agency, Research Triangle Park, NC, April 1985.
20 B.A. Tichenor and M.A. Palazzolo, Destruction of Volatile Organic Compounds via Catalytic Incineration, Env. Prog., 6 (1987) 172.
21 Y.F.Y. Yao and J.T. Kummer, J. Catal., 28 (1973) 124.
22 C.F. Cullis, D.E. Keene and D.L. Trimm, J. Catal., 19 (1970) 378.
23 S. Balasubramanian and D.S. Viswanath, Ind. Eng. Chem. Fundam., 14 (1975) 158.
24 I.S. Jaswal, R.F. Mann, J.A. Junsola and J. Downie, Can. J. Chem. Eng., 47 (1969) 284.
25 P. Mars and D.W. van Krevelen, Special Supplement to: Chem. Eng. Sci., 3 (1954) 41.

NOTICE

This document has been reviewed in accordance with U.S. Environmental Protection Agency policy and approved for publication. Mention of trade names or commercial products does not constitute endorsement or recommendation for use.

This article documents research that was conducted under the auspices of the U.S. Environmental Protection Agency (USEPA). As an arm of the government, the USEPA has a paid up, non-exclusive, irrevocable, worldwide license to reproduce, prepare derivative works, and distribute to the public all of the material contained herein, and to grant others acting on its behalf the right to do so. The USEPA grants to the National Technical Information Service, Department of Commerce, the right to act as its agent in the distribution of this material.